ACS APPLIED MATERIALS & INTERFACES

Research Article

www.acsami.org

Interfacial Effects of the CuO/GO Composite to Mediate the Side Reactions of *N,N*-Dimethylformamide Fragments

Sai Zhang,[†] Wei Gao,[†] Jing Li,[†] Xuemei Zhou,[†] and Yongquan Qu*[,†,‡]

[†]Center for Applied Chemical Research, Frontier Institute of Science and Technology, Xi'an Jiaotong University, Xi'an 710049, China

[‡]State Key Laboratory for Mechanical Behavior of Materials, Xi'an Jiaotong University, Xi'an 710049, China

Supporting Information

ABSTRACT: The interface between nanocatalysts and graphene oxide (GO) has been found to play a crucial role in enhancing the catalytic activity and improving the selectivity of amination reactions in *N,N*-dimethylformamide (DMF). The composite catalysts of CuO/GO used for the catalytic coupling of aryl halides with amines in DMF can completely inhibit the side reaction between the aryl halides and fragments of DMF. With identical amounts of Cu-catalysts, the conversion of iodobenzene and the selectivity for the target product reached 100% when CuO/GO composite catalysts were employed, while these results were 70.3 and 42.8%, respectively, when CuO catalysts were used alone. Experimental evidence confirms that the interfacial effect of CuO/GO is the origination of the improved performance of composite catalysts, which has been found to efficiently transfer fragments of DMF to GO and avoid unexpected side reactions during the catalytic process.

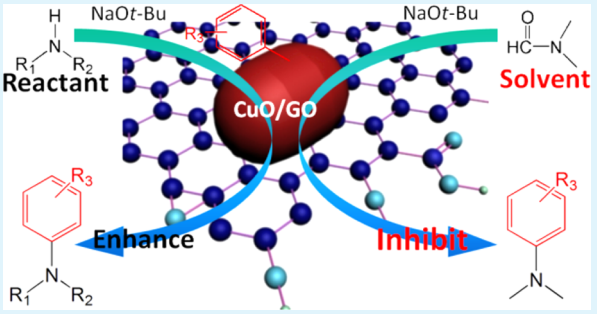

KEYWORDS: *C−N coupling reaction, interfacial effect, CuO, graphene oxide, heterogeneous catalysis*

1. INTRODUCTION

The formation of C−N bonds has attracted considerable intention in the field of organic catalysis due to the propensity of nitrogen-containing compounds to function as potential biologically active molecules, pharmaceutical agents, and novel hybrid materials.[1−4] Various approaches including reductive amination,[5,6] Ullmann coupling,[7,8] and Buchwald−Hartwig coupling[9−11] have been successfully devised to foment C−N coupling. Generally speaking, both noble metal (Pd) and transitional metal (Cu, Fe, Ni) molecular catalysts have been commonly employed to accomplish this with the assistance of bases and additives.[12−15] Especially, ligand chelation with the metal is critical for the C−N coupling reaction.[16,17] Hence, separation of products from the reaction solution and recycling of the metal catalysts and prerequisite ligands become a challenge for the coupling reaction.

The features of the heterogeneous catalytic systems, including easy product separation, efficient recyclability of catalysts, and minimization of chemical waste, can overcome the limitations of their homogeneous catalysis counterpart. Recently, it has been recognized that the utilization of the heterogeneous catalysts based on the first-row transition metals can result in "green" and cost-effective processes.[18] As an example, Pd- and Cu- based heterogeneous catalysts have been investigated for use in the C−N coupling reaction.[19−21] The C−N coupling reaction can be performed in a wide variety of solvents including toluene, tetrahydrofuran (THF), 1,4-dioxane, *N,N*-dimethylacetamine (DMA), dimethyl sulfoxide (DMSO), and even water.[10,17,22−24] As reported, the homogeneous C−N coupling reactions catalyzed by Pd can be accelerated in polar solvents in many instances.[25,26] Although *N,N*-dimethylformamide (DMF) is an excellent polar solvent for various chemical reactions, the heterogeneous C−N coupling reaction has seldom been performed in DMF.[27,28] This can be partly explained by the increasing side reactions that occur with the fragments of DMF and the consequential low yield and poor selectivity. Hence, the performance of DMF in the heterogeneous amination reaction may be far from satisfactory. To the best of our knowledge, detailed investigations on the solvent effects of DMF for the amination reaction have not been reported, despite the numerous advantages offered by DMF for organic reactions.

In this work, low yields and poor selectivity of the amination reaction between aryl iodide and pyrrole were observed when the reactions were catalyzed by CuO particles in DMF. The byproduct was originated from the side reaction between aryl iodide and dimethylamine fragments from DMF. To our surprise, a composite catalyst composed of CuO and graphene oxide (GO) nanosheets not only enhanced the catalytic activity of this reaction but also completely suppressed the side reaction of the C−N coupling reaction in DMF. Such enhanced activity and improved selectivity are attributed to the existence of the interface between the metal oxide and GO nanosheets. Control experiments indicated that composites' interface efficiently

Received: August 28, 2014
Accepted: December 1, 2014
Published: December 1, 2014

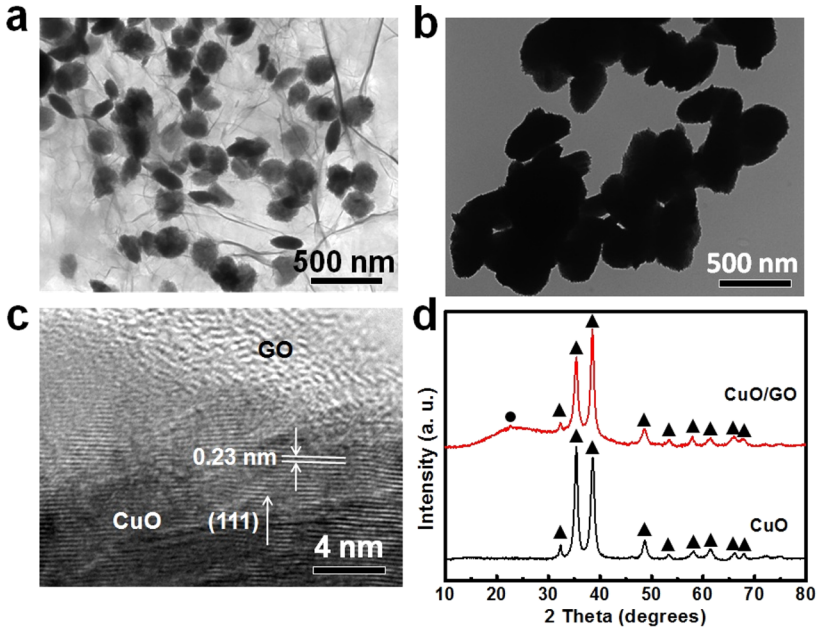

Figure 1. (a) TEM image of CuO/GO composites; (b) TEM image of CuO catalysts; (c) high-resolution TEM image of CuO/GO composite; and (d) XRD patterns of CuO and CuO/GO catalysts.

transferred the fragments of DMF to the GO nanosheets and completely inhibited the pathway between the fragments and aryl iodide during the process of the amination reaction. X-ray photoelectron spectroscopy (XPS) analyses on the fresh and used catalysts further confirmed the proposed mechanism. Such an interfacial effect may provide a novel approach to improving the selectivity of many important organic catalytic reactions.

2. EXPERIMENTAL SECTION

All chemicals (AR grade) were used as received. Deionized water with a resistivity of 18.2 MΩ cm was used for all experiments. All glassware was thoroughly washed using aqua regia (a volume ratio of 1:3 of concentrated nitric acid and hydrochloric acid) to avoid any possible contamination. Following the acid wash, the glassware was triple rinsed with deionized water.

2.1. Synthesis of GO Nanosheets. Graphite oxide (GO) nanosheets were synthesized from natural graphite powder according to the modified Hummers' method.[29] Typically, 3.0 g graphite and 1.5 g $NaNO_3$ were mixed in 70 mL of concentrated sulfuric acid (98%) under vigorous stirring at room temperature. The mixture was cooled to 0 °C in an ice−water bath. Under vigorous stirring, 9.0 g of $KMnO_4$ was added slowly to keep the temperature of the suspension below 20 °C. After the formation of a thick paste, 140 mL of water was added slowly. The solution was kept stirring at 90 °C for 15 min. Then, 500 mL of water and 20 mL of H_2O_2 (30%) were added in a sequence. The mixture was filtered and washed with a HCl solution (250 mL, 1.2 M) and then with copious amounts of water to remove the salts and acid. The resulting solid was dispersed in water by ultrasonication for 1 h to prepare a GO aqueous dispersion. The dispersion was centrifuged at 4000 rpm to remove the aggregates. Finally, the brown dispersion product was purified by dialysis for 1 week to remove any remaining impurities and stored with a concentration of 2 mg/mL for the future use.

2.2. Synthesis of CuO/GO and CuO Catalysts. The CuO/GO composite was prepared by a facile wet chemical approach. In a typical synthesis, 50 mL of 24 mM $Cu(CH_3COO)_2{\cdot}H_2O$ aqueous solution was added to 50 mL of GO aqueous solution (2 mg/mL) under vigorous magnetic stirring. After 30 min, 50 mL of 0.12 M hexamethylenetetramine (HMT) was added. The reaction was maintained at 100 °C for 2 h. Then, the reaction solution was naturally cooled to room temperature. The catalysts were separated by centrifugation, alternately washed three times with copious amount of water and ethanol and then dried at 60 °C for 12 h. The CuO catalysts were synthesized using the same procedure, but in the absence of GO nanosheets.

2.3. Characterization of the Catalysts. X-ray diffraction (XRD) patterns with diffraction intensity versus 2θ were recorded in a Shimadzu X-ray diffractometer (Model 6000) using Cu K_α radiation. Transmission electron microscopic (TEM) measurements were conducted on the samples using an Hitachi HT-7700 field-emission transmission electron microscope with an accelerating voltage of 120 kV. XPS measurements were carried out with an ultrahigh vacuum apparatus equipped with a monochromatic Al Kα X-ray source and a high resolution Thermo Fisher Scientific analyzer. The CuO content was determined by inductively coupled plasma optical emission spectroscopy (ICP-OES, Agilent 7500ce).

2.4. Catalytic Test. The C−N coupling reactions were carried out in clean glassware under ambient conditions in the presence of catalysts. In a typical procedure for coupling aryl halides with amines, the Cu-catalyst, aryl halides (1 mmol), amines (1.2 mmol), and base (3 mmol) were added into solvents (4 mL). The reaction was then heated to 120 °C and kept at this temperature for the desired time. After the reaction, the solution was cooled to room temperature naturally. The catalysts were separated from the reaction solution by centrifugation. After mixing the supernatant solution with deionized water (20 mL), the products were extracted with 6 mL of ethyl acetate twice. The ethyl acetate phase was purified on a microcolumn filled with silica gel and anhydrous sodium sulfite. Finally, the products were analyzed by GC-MS (Agilent 7890A GC and 597C MS with the column of HP-5MS). Dodecane was used as the internal standard. The calculations of the conversion and selectivity of the C−N coupling reaction were shown in Supporting Information.

3. RESULTS AND DISCUSSION

3.1. Characterization of CuO and CuO/GO Catalysts. We adopted a well-reported procedure; the synthesis of GO nanosheets involved the oxidation of graphite and subsequent exfoliation of graphite oxide into individual GO nanosheets. The typical SEM image, XRD and FT-IR spectrum of GO nanosheets are presented in Figures S1−S3 (Supporting Information) and are consistent with the previous report.[30] The composite catalysts of CuO/GO were prepared by a facile

Table 1. Preliminary Results for the C−N Coupling Reactions between Iodobenzene and Pyrrole[a,b]

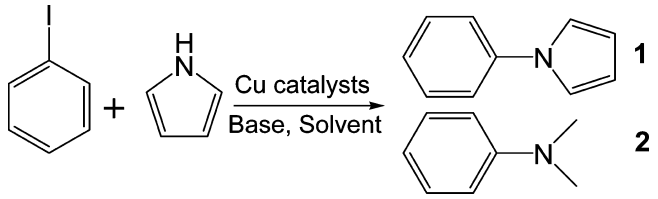

entry	catalysis	solution	base	time (h)	selectivity (%)	conversion (%)
1	CuO	THF	NaO*t*-Bu	8		0
2	CuO	Toluene	NaO*t*-Bu	8		trace
3	CuO	DMSO	NaO*t*-Bu	8	100	60
4	CuO	DMF	NaO*t*-Bu	8	42.1	100
5	CuO	DMF	K_2CO_3	8		trace
6	CuO	DMF	Et_3N	8		trace
7	CuO power	DMF	NaO*t*-Bu	8	46.2	100
8	CuO nanoparticles	DMF	NaO*t*-Bu	8	40.0	100
9	CuO/GO	DMF	NaO*t*-Bu	8	100	100
10	CuO	DMF	NaO*t*-Bu	5	42.8	70.3
11	CuO/GO	DMF	NaO*t*-Bu	5	100	99.4

[a]Unless otherwise noted, the reaction conditions are iodobenzene (1 mmol), pyrrole (1.2 mmol), base (3 mmol), the amount of catalysts (CuO 8 mg or CuO/GO 16 mg), 4 mL of solvent, and 120 °C. [b]The conversion of iodobenzene and corresponding selectivity to product **1** are determined by GC-MS with an internal label dodecane.

one-step wet chemistry approach, as described in the Experimental Section. The TEM image (Figure 1a) indicates that the as-synthesized CuO nanoparticles anchored on the surface of GO nanosheets have an olivary shape with an average length of 200 nm. In contrast, CuO nanoparticles synthesized in the absence of GO nanosheets exhibit the similar morphology with a larger size of ∼500 nm (Figure 1b). The clear lattice fringes in high resolution TEM image of the composite (Figure 1c) exhibit the good crystallinity of the as-prepared CuO on GO nanosheets. The measured planar spacing of 0.23 nm is in good agreement with the (111) crystalline plane of the monoclinic CuO. The phase of the as-prepared CuO and CuO/GO catalysts were further confirmed by the XRD analysis. As shown in Figure 1d, the XRD spectra clearly show the CuO phase with a monoclinic symmetry (PDF # 48-1548).[31−33] Both catalysts exhibit similar diffraction patterns with the exception of an additional broad peak centered at 26° for CuO/GO, which can be assigned to the GO and indicate the presence of GO nanosheets in the composite catalysts. The exact amount of loading of CuO in the composite catalysts was determined by ICP-OES and was found to be 50.78%, which was close to the theoretical value of 48.9%.

3.2. Optimization of C−N Coupling Reaction of Iodobenzene and Pyrrole. Previous studies have reported that the C−N coupling reaction occurs easier in polar, aprotic solvents such as DMF and DMSO in comparison to less polar solvents.[17] Herein, the C−N coupling reaction of iodobenzene and pyrrole was performed in an effort to optimize the reaction conditions. The results are presented in entries 1−11 (Table 1). The C−N coupling reactions catalyzed by CuO catalysts were more efficient in DMSO (entry 3) and DMF (entry 4) than those in THF and toluene (entries 1 and 2), which was consistent with previous reports.[20,22] Moreover, the conversion of iodobenzene in DMF attained 100% after 8 h of reaction, which was much higher than the 60% conversion that occurred in DMSO under similar conditions. It was also found that the selected base played an important role in the C−N coupling reaction. It was found that NaOt-Bu promoted the C−N coupling reactions (entry 4) effectively, which produced a 100% conversion within 8 h. By contrast, barely any catalytic activity was observed for CuO catalysts if K_2CO_3 (entry 5) or Et_3N (entry 6) was used as the base.

The results indicate that DMF is the best solvent for conversion of the reactants. However, GC-MS analysis of the products in DMF clearly showed the coexistence of the target product *N*-phenylpyrrole **1** and a byproduct *N*,*N*-dimethylaniline **2**. The selectivity of the target product **1** was only 42.1% (entry 4). A selectivity of 46.2% was observed when the C−N coupling reaction was catalyzed by a commercial CuO power (Alfa Aesar, entry 7), and a target compound selectivity of 40.0% resulted when the reaction was catalyzed by CuO nanoparticles synthesized according to a previous report (entry 8).[21] Notably, 100% conversion of the reactants and 100% selectivity of product **1** were realized when CuO/GO was employed as the catalyst for C−N coupling reaction in DMF (entry 9). The results indicate that the presence of the GO nanosheet in the composite catalysts can effectively suppress the side reaction. We also tracked the conversion and the selectivity of the C−N coupling reaction as a function of reaction times for the composite catalysts. As presented in Figure S4 (Supporting Information), the conversion of iodobenzene and the selectivity toward product **1** (entry 11) were maintained at 99.4 and 100%, respectively, when the reaction time was set at 5 h. By contrast, under the same conditions, the C−N coupling reaction catalyzed by CuO catalysts (entry 10) reached only 70.3% conversion of iodobenzene and 42.8% selectivity for product **1** after 5 h reaction. Therefore, the presence of GO nanosheets not only enhanced the catalytic activity of CuO for C−N coupling reaction but also improved the selectivity of the target product in DMF.

3.3. Catalytic Mechanism of CuO/GO in DMF system. Conversion and selectivity are two important factors for evaluating the efficiency of organic catalytic systems. GO- or graphene-based catalysts have been found to be highly selective for phenylacetylene hydrogenations and the Heck coupling

reaction.[34,35] The improved selectivity has been attributed to the preferentially absorbed conjugated reactants to GO or graphene. Herein, the composite of CuO/GO can completely depress the side reaction of the C−N coupling in DMF. To the best of our knowledge, this is the first example where the interfacial effect of metal oxide/GO nanosheet composites can effectively depress the side reaction and realize high selectivity for the target product. To understand the functions of GO nanosheets, control experiments were performed to study the mechanism of the C−N coupling reaction catalyzed by CuO/GO composite and roles of GO nanosheets.

It has previously been shown that DMF can be utilized as the reaction precursor for aminocarbonylation and cyanation by CuO catalysts.[27,28,36,37] From the structural features of product **2**, the formation of the byproduct **2** can be ascribed to the C−N coupling reaction between iodobenzene and the dimethylamine fragments of DMF under the reaction conditions. To validate this hypothesis, we conducted parallel experiments to entry **4** in the absence of pyrrole. When CuO was used as the catalysts, the reaction generated three products, as shown in Figure 2. Product **3** is the intermediate compound between

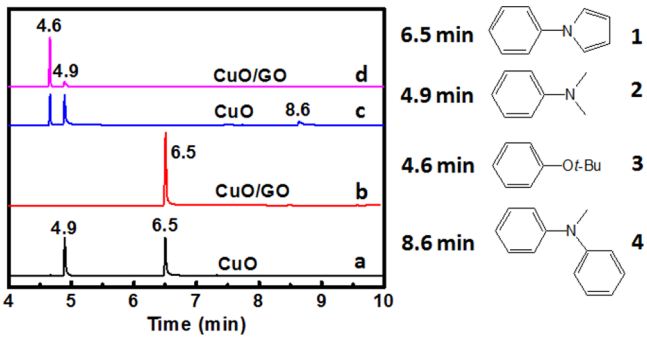

Figure 2. GC-MS results for the C−N coupling reactions. (a) Amination reaction between iodobenzene and pyrrole catalyzed by CuO in DMF. (b) Amination reaction between iodobenzene and pyrrole catalyzed by CuO/GO in DMF. (c) Chemical reaction in DMF in the presence of CuO catalysts and iodobenzene. (d) Chemical reaction in DMF in the presence of CuO/GO catalysts and iodobenzene. Product **1** is the target product, and **2** is the byproduct. In the absence of pyrrole, product **3** is the intermediate compound between iodobenzene and NaO-*t*Bu for the coupling reaction. Products **2** and **4** are generated from coupling iodobenzene with the DMF fragments.

iodobenzene and NaO-*t*Bu from the coupling reaction. Products **2** and **4** were generated from the coupling reaction between iodobenzene and DMF fragments, with a selectivity of 55.7 and 7.3%, respectively. By contrast, the parallel experiment to entry 11 in the absence of pyrrole exhibited two products (**2** and **3**) and the selectivity of byproduct **2** was only 10.2%. Hence, the side reaction of C−N coupling reaction between iodobenzene and pyrrole in DMF results from the fragments of DMF under the specified reaction conditions. While the CuO/GO composite can efficiently inhibit the side reactions of DMF, with the addition of pyrrole, the amination reaction between iodobenzene and DMF fragments was completely suppressed (entry 11). By contrast, byproduct **2** was still observed when CuO was employed as the catalyst in the coupling reaction (Figure 2).

The presence of GO nanosheets is the critical factor in suppressing the side reaction of the C−N coupling reaction. Although the C−N coupling reaction cannot occur with pure GO nanosheets (entries 12 and 13, Table 2), it is still difficult to differentiate such a function from the interfacial effect of

Table 2. C−N Coupling Reaction of Iodobenzene and Pyrrole with Different Catalysts[a,b]

entry	catalyst	GO (mg)	time (h)	selectivity (%)	conversion (%)
12	0	5	5	0	0
13	0	15	5	0	0
14	CuO 5 mg	0	5	42.96	57.2
15	CuO 5 mg	5	5	53.43	57.08
16	CuO 5 mg	5	12	56.04	100
17	CuO 5 mg	15	12	58.97	100
18	CuO/GO 5 mg	0	8	53.85	95.75
19	CuO/GO 10 mg	0	8	68.28	99.28
20	CuO/GO 15 mg	0	8	88.9	100
21	CuO/GO 20 mg	0	8	98.8	100

[a]Unless otherwise noted, the reaction conditions are iodobenzene (1 mmol), pyrrole (1.2 mmol), NaO−*t*Bu (3 mmol), 4 mL of solvent, and 120 °C. [b]The conversion of iodobenzene and corresponding selectivity to product **1** is determined by GC-MS with an internal label dodecane.

CuO/GO composite or GO nanosheets alone. To elucidate the mechanism, control experiments presented in Table 2 were performed. Because the selectivity of the C−N coupling reaction catalyzed by CuO was poor and this improved in the presence of GO nanosheets, a controlled amount of free-standing GO nanosheets were added to the reaction solutions catalyzed by CuO (entries 14−17). In the absence of GO nanosheets, the conversion of iodobenzene and the selectivity for product **1** were 57.2 and 42.9% for 5 h of reaction (entry 14), respectively. After the addition of 5 mg of GO nanosheet (entry 15), the conversion of iodobenzene was 57.1%, indicating that the catalytic activity of the CuO catalyst cannot be enhanced by free-standing GO nanosheets. At the same time, the selectivity for the target product increased from 42.9 to 53.4%. When the coupling reaction was performed for 12 h in the presence of 5 mg GO nanosheets (entry 16), the conversion of iodobenzene reached 100%. However, the selectivity for product **1** was only 56.04%, similar to that for short reaction time (entry 15). When 20 mg of GO nanosheets was introduced into the reaction mixture (entry 17), product **1** selectivity increased to 58.97%, which was not significantly improved, indicating that the free-standing GO nanosheets or a physical mixture of CuO and GO nanosheets cannot suppress the side reaction of the C−N coupling reaction in DMF.

In parallel experiments (entries 18−21), the selectivity for target product **1** was significantly increased from 53.8 to 68.3, 88.9, and 98.8% when the dosage of CuO/GO composites was increased from 5 to 10, 15, and 20 mg, respectively. Because the four C−N coupling reactions exhibited similar conversion rates of iodobenzene, a strong correlation between the amount of CuO/GO catalysts used and the selectivity toward product **1** was observed. Apparently, the interface of CuO and GO nanosheets is responsible for the suppression of the side reaction originating from DMF in the C−N coupling reaction. A sufficient quantity of the interface of the CuO and GO nanosheets will completely suppress the side reaction between iodobenzene and fragments of DMF. A proposed reaction mechanism for the improved selectivity of the C−N coupling reaction catalyzed by CuO/GO in DMF is illustrated in Figure 3.

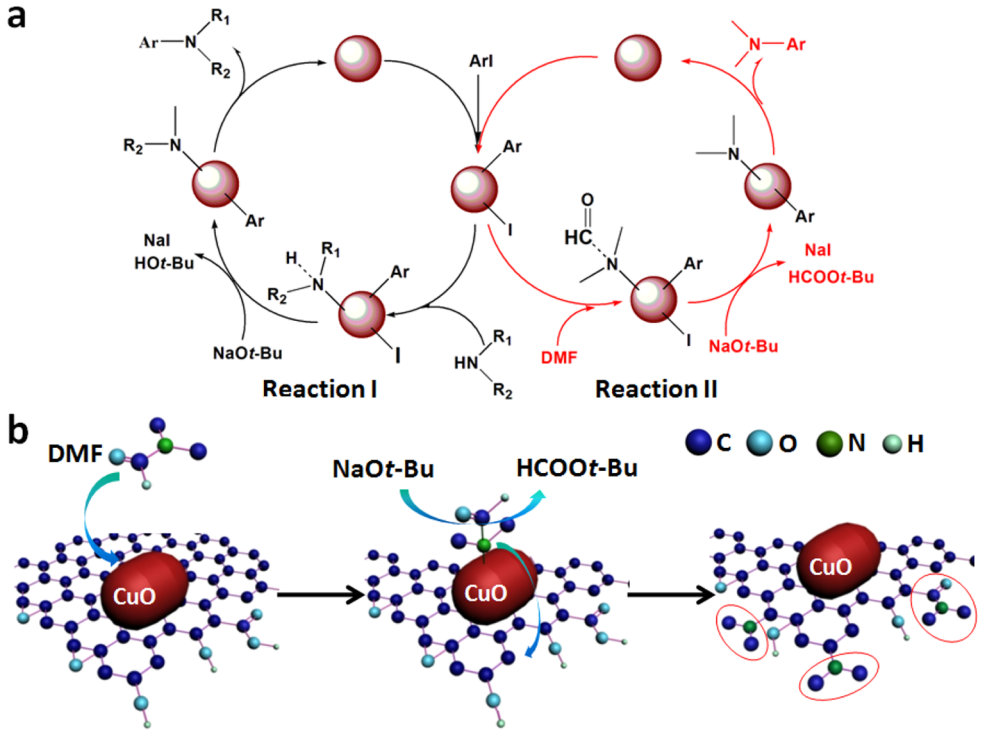

Figure 3. (a) Proposed amination reaction mechanisms with CuO catalyst in DMF and (b) schematic for chemical transfer of the dimethylamine fragments from the surface of CuO to the GO nanosheets.

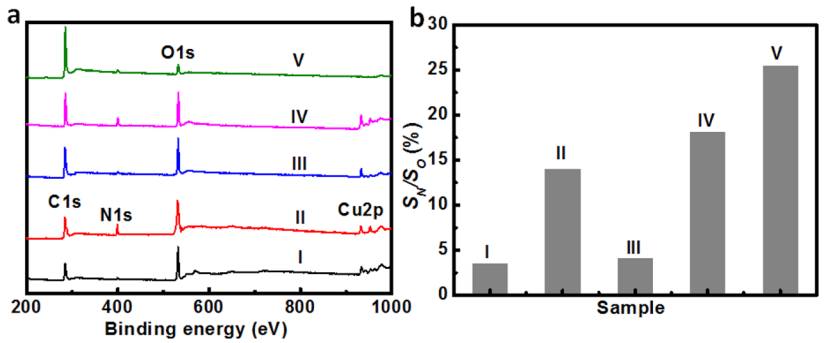

Figure 4. XPS characterization of the fresh CuO/GO and used CuO/GO catalysts. (a) The XPS survey spectra, (b) the ratio of integral area of N_{1s} peak to integral area of O_{1s} peak (S_N/S_O) for different catalysts. **I** is the freshly prepared CuO/GO catalyst. **II** is the used CuO/GO catalyst after amination between iodobenzene and pyrrole in DMF. **III** and **IV** are the CuO/GO catalysts treated with pure pyrrole and DMF at reaction temperature, respectively. **V** is GO sheets obtained from the used CuO/GO catalyst after removing CuO by HCl.

Similar to previous reports, the amination of aryl iodide catalyzed by CuO nanoparticles occurs via an oxidative addition followed by a reductive elimination process (Figure 3a). Reaction **I** is the expected C−N coupling reaction and the products are the anticipated arylamines. Reaction **II** results in the formation of byproduct **2** resulting from the coupling reaction between iodobenzene and DMF. Because employment of DMF as a reaction precursor in the Cu-catalyzed amination and cyanation reaction had resulted in important achievments in the field,[28,36,37] it is not surprising to observe the low catalytic selectivity of the C−N coupling reaction in DMF despite the higher reaction rates. In the case of CuO/GO catalyst, the high selectivity for the target product indicates that reaction pathway **II** between the generated fragments of DMF and aryl iodide is blocked. Previous studies have revealed that DMF can be decomposed to the strong electron denoting group dimethylamine at high temperature, which is an effective approach for preparing nitrogen doped GO nanosheets.[38,39] The decomposed dimethylamine can be introduced into the GO to yield 1,2-amino alcohol or amide by employing the epoxy group, −OH, −COOH or the structural defects of GO sheets.[40,41] In the case of the C−N coupling reactions catalyzed by CuO/GO, the reaction between the dimethylamine fragments and GO nanosheets is extant, leading to the immediate chemical transfer of dimethylamine fragments from the surface of the CuO to the GO nanosheets (Figure 3b). Therefore, reaction pathway **II** is interrupted and the coupling reaction of iodobenzene with the DMF fragments is inhibited. However, this chemical transfer process cannot occur for the CuO catalysts alone or the physical mixture of CuO and GO nanosheets. The generated fragments of DMF must stay on the surface of CuO and subsequently couple with iodobenzene. Therefore, the addition of free-standing GO nanosheets into the catalytic system cannot effectively suppress the side reaction, which is consistent with entries 14−17 in Table 2. The correlation between the amount of CuO/GO

Table 3. CuO/GO Catalyzed N-Arylation of Pyrrole with Various Aryl Halides[a,b]

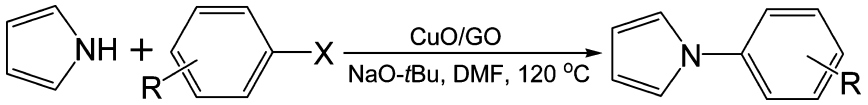

Entry	Aryl halides	Product	Time (h)	Selectivity (%)	Conversion (%)
22	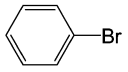	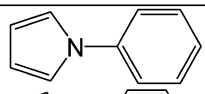	12	94.2	100
23	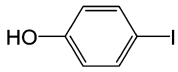	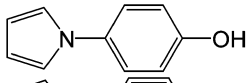	6	100	84.8
24	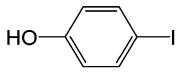	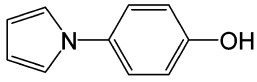	12	100	100
25	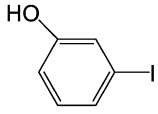	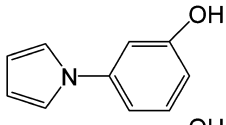	6	100	85.4
26	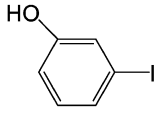	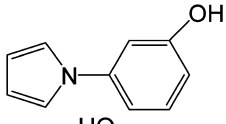	12	100	100
27	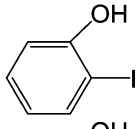	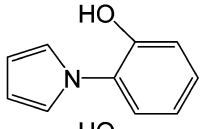	6	92.3	85.1
28	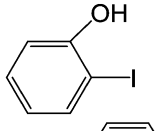	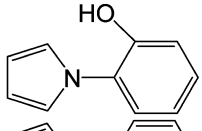	12	92.1	100
29	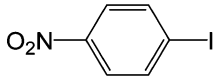	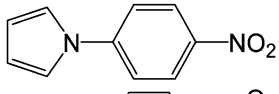	6.5	100	100
30	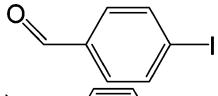	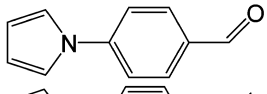	6.5	100	99.7
31	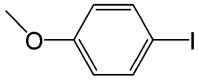	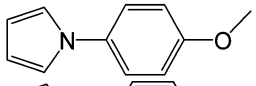	6.5	100	100
32	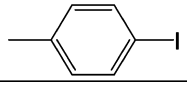	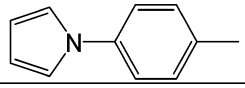	6.5	97.5	98.7

[a]All reactions were performed with 1 mmol of aryl halides, 1.2 of mmol pyrrole, and 3 of mmol of NaO-*t*Bu in 4 mL of DMF at 120 °C. The amount of CuO/GO composite catalysts was 20 mg. [b]The conversion of iodobenzene and selectivity are determined by GC-MS with an internal label dodecane.

catalysts and the reaction selectivity further confirms the interfacial effect of the composite for improving the selectivity of the C−N coupling reaction.

To better understand the reaction mechanism, the XPS was employed to study the chemical states of the catalysts during the catalytic process. The survey XPS spectra of the fresh CuO/GO, used CuO/GO, and used CuO/GO after removing CuO by acidic etching were recorded (Figure 4a). The ratio of integral area of N_{1s} peak to integral area of O_{1s} peak (S_N/S_O) was calculated as an indicator of possible reactions in the C−N coupling reaction system (Figure 4b). For the used CuO/GO catalysts, the S_N/S_O was 14.1%, which was much higher than that (3.6%) of the freshly prepared CuO/GO composites. This indicates the successful N-doping of GO nanosheets after the C−N coupling reaction. To determine the sources of nitrogen introduced into GO nanosheets, a control experiment using CuO/GO catalysts in pure DMF or pyrrole, individually, were performed under the same reaction conditions. In the case of pyrrole, the S_N/S_O (4.2%) was slight higher than that of the fresh catalysts. By contrast, the value of S_N/S_O (18.1%) for the catalysts in DMF was much higher than that of pyrrole, indicating that the interface of CuO/GO was more favorable for the transfer of the decomposed fragments of DMF to GO nanosheets. Therefore, the increased N fraction of the catalysts after the C−N coupling reactions is believed to originate from the adsorbed decomposed DMF rather than pyrrole. After the removal of the CuO from the used CuO/GO catalysts and its subsequent washing with copious quantities of water, the S_N/S_O increased to 25.5%, which could be attributed to the decreased amount of oxygen after the removal of CuO. The increased value of S_N/S_O further confirmed that the fragments of DMF were transferred to GO with the assistance of the interface of CuO and GO other than CuO. Under the amination reaction conditions, both the amines and fragments of DMF can affiliate

Table 4. CuO/GO Catalyzed N-Arylation of Various Amines with Iodobenzene[a,b]

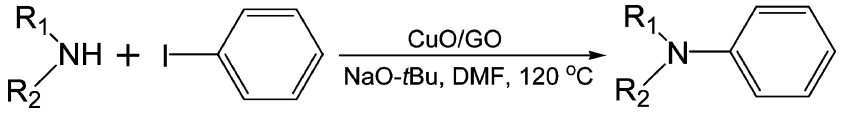

Entry	Amine	Product	Time (h)	Selectivity (%)	Conversion (%)
33	$CH_3(CH_2)_3NH_2$	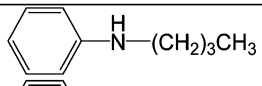	8	100	100
34	$CH_3(CH_2)_7NH_2$	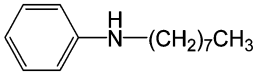	8	70.3	74.6
35	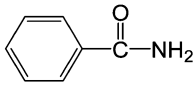	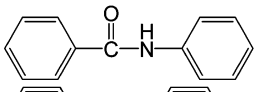	12	100	97.5
		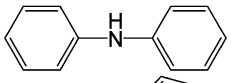		46.8	
36	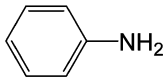	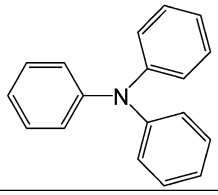	8	53.2	100

[a]All reactions were performed with 1 mmol of iodobenzene, 1.2 mmol of amine, and 3 mmol of NaO-*t*Bu in 4 mL of DMF at 120 °C. The amount of CuO/GO composite catalysts was 20 mg. [b]The conversion of iodobenzene and selectivity are determined by GC-MS with an internal label dodecane.

with the surface of CuO. Due to the efficient transfer of the fragments of DMF to GO by the interface of CuO/GO, the side reaction can be effectively avoided. The absorbed amines on CuO tend to react with aryl halides, leading to the high selectivity of the C−N coupling reactions. The proposed mechanism is consistent with the experimental observations.

The reusability of CuO/GO composite catalysts is shown in Figure S5 (Supporting Information). Although the conversion of iodobenzene could attain 100%, the selectivity of the product **1** gradually decreased from 100 to 66.8% after three reaction cycles. These results further confirmed the proposed reaction mechanism since the used CuO/GO composite catalysts had fewer available sites to accept the DMF fragments. Therefore, the transfer of the DMF fragments became more difficult which decreased the reaction selectivity for the product **1**. Decreasing the size of CuO on GO nanosheets can increase the interface of the composites, which may improve the catalytic selectivity during the reuse of the catalysts.

3.4. Extension of Scope. Having established the optimal reaction conditions and an understanding of the reaction mechanism, the test protocol was extended to various aryl halides and substituted pyrroles to verify the scope of catalytic system, and these results are listed in Table 3. The coupling of bromobenzene with pyrrole proceeded smoothly to yield the target product with 100% conversion of bromobenzene and 94.2% selectivity within 12 h (entry 22), although the activity of bromobenzene was less than that of iodobenzene. Iodobenzene containing electron-donating hydroxyl groups at *ortho*, *meta*, and *para* positions also successfully coupled with pyrrole in excellent yields and good selectivity (entries 23−28). The reactions were completed within 12 h, indicating the low activity of the electron-donating substituted iodobenzene for the coupling reactions. Nevertheless, all reactions approached the 100% selectivity for the desired products, except *ortho*-substituted aryl iodides, which produced a selectivity of 92.3% due to the steric hindrance of the *ortho*-substituent. Iodobenzene with either weak electron-donating or electron-withdrawing groups also reacted with pyrrole under the specified reaction conditions and produced satisfactory conversion and selectivity (entries 29−32).

Nitrogen-containing heterocycles such as imidazole, carbazole, and indole have been widely studied in literature, but very little attention has been paid to aliphatic amines. Therefore, it was decided to extend the scope of current catalytic reaction between various primary amines and iodobenzene. The coupling reaction between *n*-butylamine and iodobenzene catalyzed by CuO/GO composite was successfully performed using the current approach. Both the conversion of reactants and selectivity for the target product attained 100% (Table 4, entry 33). However, the reaction of *n*-heptylamine with a longer carbon chain was slower and incomplete after 8 h, yielding 74.6% conversion of iodobenzene and 70.3% selectivity (entry 34). Benzamide was another type of common amination reagent that also underwent a successful coupling to afford a 100% selectivity for the target product (entry 35). The coupling reaction of aniline also yielded 100% conversion of iodobenzene without the byproduct of iodobenzene with the DMF fragments. It should be mentioned that diphenylamine (46.8%) and triphenylamine (53.2%) were produced simultaneously (entry 36). The generated diphenylamine, which was more active than aniline, could couple with iodobenzene and form triphenylamine.

4. CONCLUSION

In summary, the C−N coupling reactions with the high catalytic activity and selectivity were successfully achieved in DMF by using a CuO/GO composite catalyst. The presence of GO was very important for the promoted catalytic activity of CuO/GO catalysts. GO nanosheets functioned as the support for CuO particles and enhanced the catalytic activity of CuO

for the coupling reaction. Notably, the catalytic selectivity of the coupling reaction for the target product was significantly improved, attaining 100% by using CuO/GO catalysts. Poor selectivity of the coupling reactions catalyzed by CuO was observed as a result of the competing reaction of the dimethylamine fragments from DMF. Mechanistic study indicated that the interface of CuO and GO can transfer the fragments of DMF to GO nanosheets and subsequently block the reaction pathway between the DMF fragments and aryl halides. We trust that this interfacial effect of catalysts and GO nanosheets might provide new opportunities for the development of novel catalysts to improve reaction selectivity for the desired products.

■ ASSOCIATED CONTENT

Supporting Information

Detailed information regarding typical SEM images, XRD and FT-IR spectra of GO nanosheets, the conversion and selectivity of coupling iodobenzene and pyrrole at different time points, and the reusability of CuO/GO composite catalysts and the calculation equations of the conversion of the reactant and the selectivity of the target product. This material is available free of charge via the Internet at http://pubs.acs.org.

■ AUTHOR INFORMATION

Corresponding Author

*E-mail: yongquan@mail.xjtu.edu.cn.

Notes

The authors declare no competing financial interest.

■ ACKNOWLEDGMENTS

We acknowledge the financial support of the NSFC (Grant 21201138). This work was also partially funded by the Ministry of Science and Technology of China through a 973-program under Grant 2012CB619401 and by the Fundamental Research Funds for the Central Universities under Grants xjj2013102 and xjj2013043. Technical support for TEM experiments was provided by the Frontier Institute of Science and Technology.

■ REFERENCES

(1) Kawano, T.; Hirano, K.; Satoh, T.; Miura, M. A New Entry of Amination Reagents for Heteroaromatic C-H Bonds: Copper-Catalyzed Direct Amination of Azoles with Chloroamines at Room Temperature. *J. Am. Chem. Soc.* **2010**, *132*, 6900−6901.

(2) Imm, S.; Bähn, S.; Zhang, M.; Neubert, L.; Neumann, H.; Klasovsky, F.; Pfeffer, J.; Haas, T.; Beller, M. Improved Ruthenium-Catalyzed Amination of Alcohols with Ammonia: Synthesis of Diamines and Amino Esters. *Angew. Chem., Int. Ed.* **2011**, *50*, 7599−7603.

(3) Matsuda, N.; Hirano, K.; Satoh, T.; Miura, M. Copper-Catalyzed Direct Amination of Electron-Deficient Arenes with Hydroxylamines. *Org. Lett.* **2011**, *13*, 2860−2863.

(4) Lyons, T. W.; Sanford, M. S. Palladium-Catalyzed Ligand-Directed C−H Functionalization Reactions. *Chem. Rev.* **2010**, *110*, 1147−1169.

(5) Koszelewski, D.; Lavandera, I.; Clay, D.; Guebitz, G. M.; Rozzell, D.; Kroutil, W. Formal Asymmetric Biocatalytic Reductive Amination. *Angew. Chem., Int. Ed.* **2008**, *47*, 9337−9340.

(6) Li, C.; Villa-Marcos, B.; Xiao, J. Metal−Brønsted Acid Cooperative Catalysis for Asymmetric Reductive Amination. *J. Am. Chem. Soc.* **2009**, *131*, 6967−6969.

(7) Monnier, F.; Taillefer, M. Catalytic C−C, C−N, and C−O Ullmann-Type Coupling Reactions: Copper Makes a Difference. *Angew. Chem., Int. Ed.* **2008**, *47*, 3096−3099.

(8) Monnier, F.; Taillefer, M. Catalytic C−C, C−N, and C−O Ullmann-Type Coupling Reactions. *Angew. Chem., Int. Ed.* **2009**, *48*, 6954−6971.

(9) Paul, F.; Patt, J.; Hartwig, J. F. Palladium-Catalyzed Formation of Carbon-Nitrogen Bonds. Reaction Intermediates and Catalyst Improvements in the Hetero Cross-Coupling of Aryl Halides and Tin Amides. *J. Am. Chem. Soc.* **1994**, *116*, 5969−5970.

(10) Fors, B. P.; Davis, N. R.; Buchwald, S. L. An Efficient Process for Pd-Catalyzed C−N Cross-Coupling Reactions of Aryl Iodides: Insight Into Controlling Factors. *J. Am. Chem. Soc.* **2009**, *131*, 5766−5768.

(11) Guram, A. S.; Buchwald, S. L. Palladium-Catalyzed Aromatic Aminations with in situ Generated Aminostannanes. *J. Am. Chem. Soc.* **1994**, *116*, 7901−7902.

(12) Jana, S.; Clements, M. D.; Sharp, B. K.; Zheng, N. Fe (II)-Catalyzed Amination of Aromatic C−H Bonds via Ring Opening of 2H-Azirines: Synthesis of 2,3-Disubstituted Indoles. *Org. Lett.* **2010**, *12*, 3736−3739.

(13) Ge, S.; Green, R. A.; Hartwig, J. F. Controlling First-Row Catalysts: Amination of Aryl and Heteroaryl Chlorides and Bromides with Primary Aliphatic Amines Catalyzed by a BINAP-Ligated Single-Component Ni (0) Complex. *J. Am. Chem. Soc.* **2014**, *136*, 1617−1627.

(14) Fors, B. P.; Watson, D. A.; Biscoe, M. R.; Buchwald, S. L. A Highly Active Catalyst for Pd-Catalyzed Amination Reactions: Cross-Coupling Reactions Using Aryl Mesylates and the Highly Selective Monoarylation of Primary Amines Using Aryl Chlorides. *J. Am. Chem. Soc.* **2008**, *130*, 13552−13554.

(15) Liang, L.; Li, Z.; Zhou, X. Pyridine N-Oxides as Ligands in Cu-Catalyzed N-Arylation of Imidazoles in Water. *Org. Lett.* **2009**, *11*, 3294−3297.

(16) Surry, D. S.; Buchwald, S. L. Biaryl Phosphane Ligands in Palladium-Catalyzed Amination. *Angew. Chem., Int. Ed.* **2008**, *47*, 6338−6361.

(17) Surry, D. S.; Buchwald, S. L. Dialkylbiaryl Phosphines in Pd-Catalyzed Amination: A User's Guide. *Chem. Sci.* **2011**, *2*, 27−50.

(18) Han, F. S. Transition-Metal-Catalyzed Suzuki−Miyaura Cross-Coupling Reactions: A Remarkable Advance from Palladium to Nickel Catalysts. *Chem. Soc. Rev.* **2013**, *42*, 5270−5298.

(19) Sá, S.; Gawande, M. B.; Velhinho, A.; Veiga, J. P.; Bundaleski, N.; Trigueiro, J.; Tolstogouzov, A.; Teodoro, O. M.; Zboril, R.; Varma, R. S. Magnetically Recyclable Magnetite-Palladium (Nanocat-Fe−Pd) Nanocatalyst for the Buchwald−Hartwig Reaction. *Green Chem.* **2014**, *16*, 3494−3500.

(20) Rout, L.; Jammi, S.; Punniyamurthy, T. Novel CuO Nanoparticle Catalyzed CN Cross Coupling of Amines with Iodobenzene. *Org. Lett.* **2007**, *9*, 3397−3399.

(21) Jammi, S.; Sakthivel, S.; Rout, L.; Mukherjee, T.; Mandal, S.; Mitra, R.; Saha, P.; Punniyamurthy, T. CuO Nanoparticles Catalyzed C−N, C−O, and C−S Cross-Coupling Reactions: Scope and Mechanism. *J. Org. Chem.* **2009**, *74*, 1971−1976.

(22) Ganesh Babu, S.; Karvembu, R. CuO Nanoparticles: A Simple, Effective, Ligand-Free, and Reusable Heterogeneous Catalyst for N-Arylation of Benzimidazole. *Ind. Eng. Chem. Res.* **2011**, *50*, 9594−9600.

(23) Su, M.; Hoshiya, N.; Buchwald, S. L. Palladium-Catalyzed Amination of Unprotected Five-Membered Heterocyclic Bromides. *Org. Lett.* **2014**, *16*, 832−835.

(24) Jiao, J.; Zhang, X.-R.; Chang, N.-H.; Wang, J.; Wei, J.-F.; Shi, X.-Y.; Chen, Z.-G. A Facile and Practical Copper Powder-Catalyzed, Organic Solvent- and Ligand-Free Ullmann Amination of Aryl Halides. *J. Org. Chem.* **2011**, *76*, 1180−1183.

(25) Kataoka, N.; Shelby, Q.; Stambuli, J. P.; Hartwig, J. F. Air Stable, Sterically Hindered Ferrocenyl Dialkylphosphines for Palladium-Catalyzed C−C, C−N and C−O Bond-Forming Cross-Couplings. *J. Org. Chem.* **2002**, *67*, 5553−5566.

(26) Zhang, Y.; César, V.; Storch, G.; Lugan, N.; Lavigne, G. Skeletion Decoration of NHCs by Amino Groups and Its Sequential Booster Effect on the Palladium-Catalyzed Buchwald−Harting Amination. *Angew. Chem., Int. Ed.* **2014**, *53*, 6482−6486.

(27) Muzart, J. *N,N*-Dimethylformamide: Much More than A Solvent. *Tetrahedron* **2009**, *65*, 8313−8323.
(28) Ding, S.; Jiao, N. *N,N*-Dimethylformamide: A Multipurpose Building Block. *Angew. Chem., Int. Ed.* **2012**, *51*, 9226−9237.
(29) Xu, Y.; Wu, Q.; Sun, Y.; Bai, H.; Shi, G. Three-Dimensional Self-Assembly of Graphene Oxide and DNA into Multifunctional Hydrogels. *ACS Nano* **2010**, *4*, 7358−7362.
(30) Marcano, D. C.; Kosynkin, D. V.; Berlin, J. M.; Sinitskii, A.; Sun, Z.; Slesarev, A.; Alemany, L. B.; Lu, W.; Tour, J. M. Improved Synthesis of Graphene Oxide. *ACS Nano* **2010**, *4*, 4806−4814.
(31) Zhang, W.; Ding, S.; Yang, Z.; Liu, A.; Qian, Y.; Tang, S. Growth of Novel Nanostructured Copper Oxide (CuO) Films on Copper Foil. *J. Cryst. Growth* **2006**, *291*, 479−484.
(32) Zarate, R. A.; Hevian, F.; Fuentes, S.; Fuenzalida, V. M.; Zúniga, A. Novel Route to Synthesize CuO Nanoparticles. *J. Solid State Chem.* **2007**, *180*, 1464−1469.
(33) Yang, X. D.; Jiang, L. L.; Mao, C. J.; Niu, H. L.; Song, J. M.; Zhang, S. Y. Sonochemical Synthesis and Nonlinear Optical Property of CuO Hierarchical Superstructures. *Mater. Lett.* **2014**, *115*, 121−124.
(34) Shao, L.; Huang, X.; Teschner, D.; Zhang, W. Gold Supported on Graphene Oxide: An Active and Selective Catalyst for Phenylacetylene Hydrogenations at Low Temperatures. *ACS Catal.* **2014**, *4*, 2369−2373.
(35) Tang, Z.; Shen, S.; Zhuang, J.; Wang, X. Noble-Metal-Promoted Three-Dimensional Macroassembly of Single-Layered Graphene Oxide. *Angew. Chem., Int. Ed.* **2010**, *49*, 4603−4607.
(36) Ding, S.; Jiao, N. Direct Transformation of *N,N*-Dimethylformamide to −CN:Pd-Catalyzed Cyanation of Heteroarenes via C−H Functionalization. *J. Am. Chem. Soc.* **2011**, *133*, 12374−12377.
(37) Li, Y.; Xie, Y.; Zhang, R.; Jin, K.; Wang, X.; Duan, C. Copper-Catalyzed Direct Oxidative C−H Amination of Benzoxazoles with Formamides or Secondary Amines under Mild Conditions. *J. Org. Chem.* **2011**, *76*, 5444−5449.
(38) Liu, Q.; Guo, B.; Rao, Z.; Zhang, B.; Gong, J. R. Strong Two-Photon-Induced Fluorescence from Photostable, Biocompatible Nitrogen-Doped Graphene Quantum Dots for Cellular and Deep-Tissue Imaging. *Nano Lett.* **2013**, *13*, 2436−2441.
(39) Ai, K.; Liu, Y.; Lu, L.; Cheng, X.; Huo, L. A Novel Strategy for Making Soluble Reduced Graphene Oxide Sheets Cheaply by Adopting An Endogenous Reducing Agent. *J. Mater. Chem.* **2011**, *21*, 3365−3370.
(40) Vinci, J. C.; Ferrer, I. M.; Seedhouse, S. J.; Bourdon, A. K.; Reynard, J. M.; Foster, B. A.; Bright, F. V.; Colón, L. A. Hidden Properties of Carbon Dots Revealed After HPLC Fractionation. *J. Phys. Chem. Lett.* **2013**, *4*, 239−243.
(41) Mei, Q.; Zhang, K.; Guan, G.; Liu, B.; Wang, S.; Zhang, Z. Highly Efficient Photoluminescent Graphene Oxide with Tunable Surface Properties. *Chem. Commun.* **2010**, *46*, 7319−7321.